K-line spectra from tungsten heated by an intense pulsed electron beam[a)]

N. R. Pereira,[1,b)] B. V. Weber,[2] J. P. Apruzese,[2] D. Mosher,[2] J. W. Schumer,[2] J. F. Seely,[2] C. I. Szabo,[2] C. N. Boyer,[3] S. J. Stephanakis,[3] and L. T. Hudson[4]
[1]*Ecopulse, Inc., P.O. Box 528, Springfield, Virginia 22150, USA*
[2]*Naval Research Laboratory, Washington DC 20375, USA*
[3]*L3-Communications, Washington, DC 20375, USA*
[4]*National Institute of Science and Technology, Gaithersburg, Maryland 20899, USA*

(Presented 19 May 2010; received 11 April 2010; accepted 3 June 2010; published online 1 October 2010)

The plasma-filled rod-pinch diode (PFRP) is an intense source of x-rays ideal for radiography of dense objects. In the PRFP megavoltage electrons from a pulsed discharge concentrate at the pointed end of a 1 mm diameter tapered tungsten rod. Ionization of this plasma might increase the energy of tungsten's $K\alpha_1$ fluorescence line, at 59.3182 keV, enough for the difference to be observed by a high-resolution Cauchois transmission crystal spectrograph. When the PFRP's intense hard bremsstrahlung is suppressed by the proper shielding, such an instrument gives excellent fluorescence spectra, albeit with as yet insufficient resolution to see any effect of tungsten's ionization. Higher resolution is possible with various straightforward upgrades that are feasible thanks to the radiation's high intensity. © *2010 American Institute of Physics.*
[doi:10.1063/1.3464268]

I. INTRODUCTION

In the mid-1970s a group at the Naval Research Laboratory (NRL) discovered the rod pinch,[1] a high-voltage, high current diode geometry that forces the electrons to pinch onto a small amount of material at the end of a thin rod. It is sketched on the left side in Fig. 1. Its high current density and small size make the rod pinch an intense source of x-rays that is ideal for radiography thanks to its small size.

Recent research motivated by the rod pinch's application to flash x-ray radiography of dense objects has led to substantial improvements over the original implementation. To date the rod pinch variant with the highest output is the plasma-filled rod-pinch,[2,3] the PFRP. In the PFRP a radially injected plasma improves electrical coupling with the generator by reducing the rod pinch's initial impedance.

At NRL the PFRP uses the pulsed power generator Gamble II. Its nominally ≃2 MeV and ≃500 kA pulse heats and ionizes the 1 mm diameter rod over a ≃3 mm length. According to simple estimates[2] the initial heating is so fast that the tungsten reaches its peak energy density, ≃2.4 MJ/cm^3, before the material expands appreciably. During the remainder of the pulse the plasma expands while it heats up to 60 eV, with W^{+16} or so as the maximum ionization state. We are interested in the effect of ionization on fluorescence.

Thermal excitation of tungsten's *M*-shell (around 1.8 keV) and higher shells is obviously impossible in a 60 eV plasma. Instead, tungsten's inner shells are excited as in the standard cold anode, mostly by the bremsstrahlung from the megavoltage electrons. The energy of the fluorescence photons increases with the atom's ionization state, hence a precise measurement of the fluorescence energy could confirm the estimates of the plasma's ionization state. Neutral tungsten's $K\alpha_1$ line at 59.3182 keV (Ref. 4) might increase 0.03 keV for xenonlike tungsten, W^{+18}.

Measuring a small ionization shift on tungsten fluorescence lines demands a hard x-ray spectrometer that covers the energy region around ≃60 keV. An initial goal for energy resolution is 0.1% or 0.06 keV. A further increase in resolution, to 0.03 keV, and the upgrading of time-integrated registration by an image plate with a diagnostic that allows temporal resolution is a challenge for the future.

This paper documents the performance to date of a Cauchois transmission crystal spectrometer[5] under development for the purpose. The spectrometer works very well for laser-produced plasmas[6,7] where *K*-transitions of heavy metals up to gold can be seen above the background. A precursor version of the present instrument discovered an anomalous ratio between the $K\alpha$ and $K\beta$ lines, in forward-directed bremsstrahlung from a cold anode in a 2 MeV linear accelerator,[8] again after taking care of the background.

Direct radiation from the cold anode or the PFRP can be suppressed sufficiently by heavy shielding in between the source and the spectrometer. Then, the dominant source of background inside the spectrometer comes from secondary scatter sources that are harder to shield from. While scattered radiation is softer than the primary bremsstrahlung, it is still too hard to suppress it further with *K*-edge filters that sometimes give a useful calibration of the energy scale. Heavier filtering of the background can give an estimate for a typical electron energy that produces the background.[9]

[a)]Contributed paper, published as part of the Proceedings of the 18th Topical Conference on High-Temperature Plasma Diagnostics, Wildwood, New Jersey, May 2010.
[b)]Electronic mail: pereira@speakeasy.net. URL: http://www.ecopulse.com.

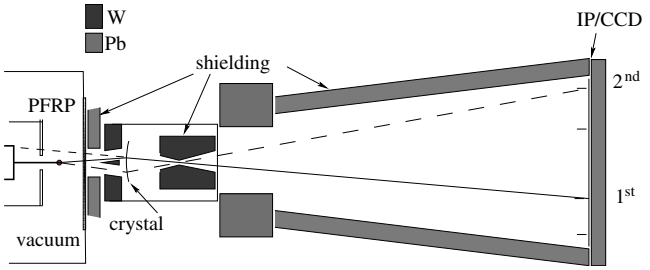

FIG. 1. (Color online) The experimental geometry. The PFRP x-ray source (red dot) is to the left, the spectrometer with its shielding is in the middle, and the image plate or CCD is to the right.

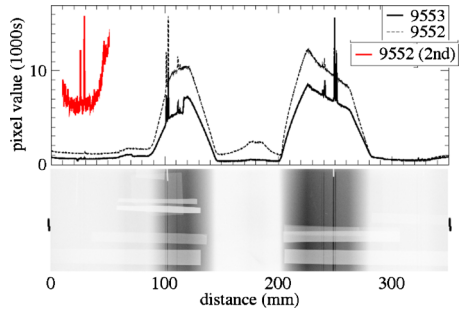

FIG. 2. (Color online) Two symmetric tungsten spectra on shot 9553. The top graph gives the line-out taken just above the upper 50 μm thick tantalum filter strip to the right, and a line-out on the nominally identical shot 9552. To the left the spectrum in second order is barely visible for shot 9552: the insert shown this part of the spectrum, multiplied 20× and with partially subtracted background.

The spectrometer's results to date are encouraging. An energy resolution of 0.06 keV seems achievable since the energy resolution is presently limited by the spatial medium, 130 μm for Fuji's BAS-SR (superior resolution) and 190 μm for BAS-MS (maximum sensitivity).[10] The resolution of a Hamamatsu dental charge-coupled device (CCD) is slightly better than BAS-SR.[11]

The radiation is intense enough that the resolution could be increased by locating the image plate farther away from the bent crystal, preferably on the Rowland circle by increasing its bending radius and possibly beyond the Rowland circle if the source is small enough.[12] Replacing the quartz $20\bar{2}3$ (or $30\bar{3}1$) crystal in the spectrometer with another crystal cut that has smaller $2d$-spacing also increases the resolution: quartz $50\bar{5}2$ has a 1.7 times smaller $2d$-spacing than the two crystal cuts mentioned, and the dispersion is correspondingly higher.

The spectrometer development effort is partly motivated by the intriguing possibility of high-density energy storage,[13] in a metastable nucleus that might give up its energy through resonance with x-rays from atomic transitions that are shifted in energy by partial ionization. While achieving resonance between atomic and nuclear levels may not have a practical application, an instrument that can discern small changes to the photon energy of K-lines from high atomic number atoms should be useful in atomic and plasma physics research. It is also a challenge.

II. EXPERIMENTAL RESULTS

Figure 1 sketches the spectrometer's geometry. The stalk to the left is the PFRP's rod: the radiation source is the red dot at its tip. The PFRP's radiation first passes through a 13 mm thick polyethylene that shields a 3 mm thick melamine vacuum barrier, and then through a 45 mm diameter aperture in a 25 mm lead radiation shield outside the vacuum. The spectrometer's crystal is quartz $20\bar{2}3$, bent on a substrate to a 965 mm radius. It is located 132 mm from the PFRP. The crystal sees the radiation through two 10 mm high and 14 mm wide apertures in a 32 mm thick tungsten shield. Inside the spectrometer are additional tungsten shields that form a 2.5 mm wide cross-over slit. X-rays between $h\nu \simeq 100$ keV and $h\nu \simeq 25$ keV are the only photons that can reach the diagnostics, on the figure's right side.

In Fig. 1 the solid line marked with 1st shows the path taken by tungsten's $K\alpha_1$ x-rays in first order. The Bragg angle is $\theta_1 \simeq 4.36°$, corresponding to $\sin\theta_1 = \lambda_{K\alpha_1}/2d$, quartz $20\bar{2}3$ plane's $2d = 0.2749$ nm and $K\alpha_1$'s wavelength $\lambda_{K\alpha_1} = 0.0209$ nm. The dashed line above the center is the same tungsten line diffracted in second order, from quartz' 4046 crystal plane and along the same path as x-rays with half the energy diffracted in first order. Tungsten pins with 1 mm diameter indicate where the first and second order $K\alpha_1$ lines appear on perfect alignment, viz., mirror-symmetric on both sides of the spectrometer's center line and 148 and 305 mm apart. The distance between the symmetric spectral lines gives the photon energy, without the uncertainty about the spectrometer's orientation in a conventional design.[14]

A 423 mm long by 200 mm high BAS-MS image plate is the standard diagnostic. It is on the Rowland circle, 965 mm from the crystal. Lead shielding limits the exposed region to a 350 mm by 90 mm area. Most plates are read with a Logos drum scanner, with 300 dots per inch nominal resolution or nominal 100 μm scan step resolution. Some later images are taken with BAS-SR image plate, read with nominal 50 μm scan step resolution by a Fuji 3000 scanner, or with a CCD with 20 μm pixel size.

The bottom part of Fig. 2 is a typical x-ray image, from Gamble II shot 9553. The larger $K\alpha_1$ and smaller $K\alpha_2$ lines close to the marking pins stick out above a substantial background. The three lower intensity $K\beta$ lines closer to the spectrometer's center are also visible. The horizontal bands in the image are from x-ray filters, 25 μm thick Hf and up to three layers of 10 μm Ta. Attenuation of the background is consistent with x-ray energies around 120 keV or so. The filters are too thin to diagnose harder x-rays, which the image plate does not see well. K-edges are absent, hence the softer part of the background is minimal.

In Fig. 2 the primary source of background is the vacuum window. This consists of 17 mm thick plastic. Photons scattered by the window can travel along the path of the $K\alpha$ x-rays diffracted by the crystal, the solid line in Fig. 1. Additional photons may scatter along the same path from the diode's steel and aluminum farther back into the diode. A later shot demonstrates that the background largely disappears when a thinner vacuum window is shielded from irradiation, and when any radiation scattered from the window is shielded off.

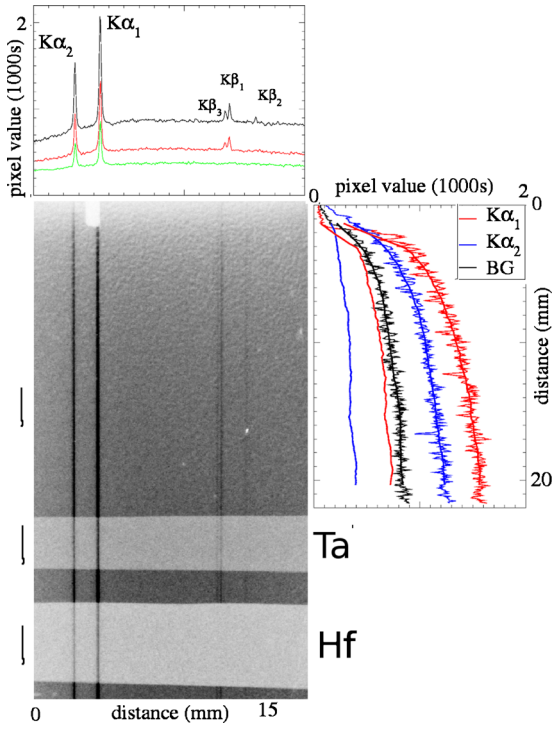

FIG. 3. (Color online) Tungsten spectrum taken with a BAS-MS image plate. The top plot shows spectra filtered with 25 μm Hf and 10 μm Ta under the unfiltered spectrum (black), the right plot is the intensity of the $K\alpha$ lines, uncorrected and corrected for the background (black).

The solid line in Fig. 2 is the average pixel value over a region suggested by the dark lines on both sides of the image, in between the filter strips. For this shot, 9553, both the lines and the background are stronger on the right side, while for a nominally identical shot, 9552, the radiation (dashed) is strongest on the left. Alignment of the spectrometer does not seem to be the cause of this asymmetry because the *K*-lines are at the same position on these two shots.

Even when the spectrometer is not perfectly aligned and the *K*-lines miss the marker pins, the distance between the *K*-lines on the two sides is almost exactly the same. Sometimes the spectral lines are farther apart at the top of the image than at the bottom 90 mm away. The reason is probably a slight tilt of the image plate with respect to the spectrometer's center line that can easily come from an estimated 0.3 mm variation in locating the image plate: it is simply pressed against the shielding. $K\alpha_1$ and $K\beta$ lines are 9.6 mm apart and differ in energy by 7.63 keV, so that 0.3 mm in between two symmetric lines translates into 0.12 keV, twice the target resolution.

Smaller variations occur when the x-ray source is off the spectrometer's center line and the *K*-lines wander away from the marking pins in response, or when the source is closer to or farther from the bent crystal. Each shot requires refurbishing Gamble II with a fresh tungsten rod, and is difficult put the spectrometer with its multiton lead shield back in exactly the same place. An uncertainty of 3 mm in axial position, the length of the source, translates into 12 μm between the *K*-lines on the Rowland circle or about 0.010 keV.

Just below the leftmost marker pin is the shadow of a BAS-SR image plate, read at 50 μm resolution. Figure 3 is

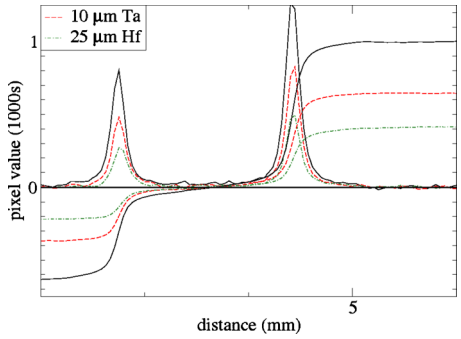

FIG. 4. (Color online) Close-up of spectral lines in Fig. 3 after removal of background, integration from the center outward, and normalization.

a 17 mm by 34 mm section of this image plate just below the marking pin, taken on the nominally identical shot 9552. The maximum intensity of a pixel in the $K\alpha_1$ line read with the Logos drum scanner at 100 μm step size resolution is about 15 000, about 1/4 of the 16-bit maximum. The BAS-SR plate read by the 16-bit Fuji 3000 scanner with 50 μm step size resolution assigns the same $K\alpha_1$ line a maximum intensity of about 2000, half the fourfold smaller value naively expected from a 4× smaller pixel.

The middle curve in the top part of Fig. 3 is the average pixel value along a band that just fits within the 0.1 mm thick tantalum filter. The lower curve is the average pixel value for the spectrum at the bottom, behind a 0.25 mm hafnium filter, while the top curve is the unfiltered spectrum just above the white spot on the $K\beta_2$ line. The averages are over bands with the same height suggested to the figure's left. The $K\beta_2$ line at 69.067 keV and 15 mm is just about visible in the unfiltered spectrum, but absent from the spectrum behind Ta: its *K*-edge at 67.416 keV suppresses $K\beta_2$ but transmits the 67.2243 keV $K\beta_1$ and 66.9514 keV $K\beta_3$ lines. Hafnium's *K*-edge at 65.351 keV filters out all the $K\beta$ lines but passes the $K\alpha$ lines. A 0.1 mm thick filter from terbium, whose shadow is barely visible to the left of the marking pin in Fig. 2, should have stopped $K\alpha_1$ photons if these had increased their energy from 59.3182 keV by more than 0.077 keV to terbium's *K*-edge at 59.390 keV (and if the filter had properly overlapped the *K*-line on this shot).

To the right side in Fig. 3 is the average pixel value along a 0.4 mm (8 pixel) strip that just covers the intense $K\alpha_1$ line, including the tungsten marking pin at the top, the average pixel value over the same strip for the less-intense $K\alpha_2$ line, and the background in between the two fluorescence lines. These have the same variation from top to bottom over a 5 mm extent, probably due to the $\simeq 1$ mm source size being cut off by the entrance aperture. Smoothing and subtracting the background produces the two lines closest to the image. The $K\alpha_2$ line is approximately half the strength of the $K\alpha_1$ line, as expected in reflection when self-filtering is absent.[8]

Figure 4 is a close-up of the two $K\alpha$ lines in the top of Fig. 3 after subtracting the background. The figure also shows the pixel value integrated over the lines, normalized to unity for unfiltered $K\alpha_1$ radiation. To make the size of the $K\alpha_2$ line obvious the integration starts in the center between the lines, and goes outward. The integrated pixel values for

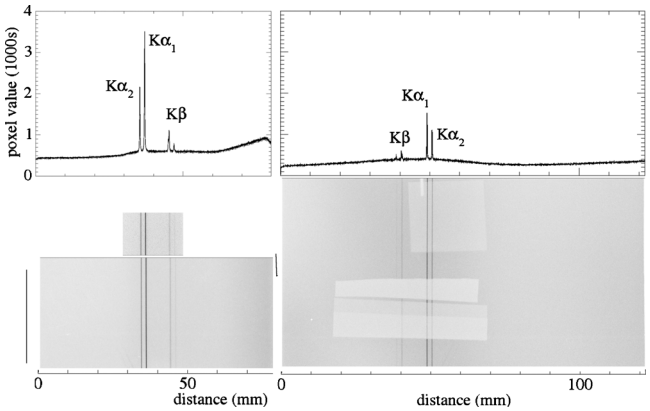

FIG. 5. Tungsten spectrum on shot 9595, registered with 70 and 130 mm wide Fuji BAS-SR image plate on both sides of the spectrometer and improved shielding. The small image to the left is from a dental CCD. The line-outs average the pixel value over the regions indicated by the bar on the sides.

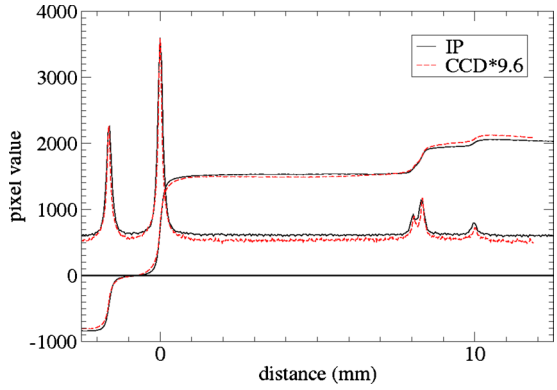

FIG. 6. (Color online) The tungsten fluorescence spectrum on Fuji BAS-SR image plate (IP) and the Hamamatsu dental CCD on shot 9595.

$K\alpha_2$ is 0.58 of the integrated pixel value for $K\alpha_1$, the same as their relative emission strengths.[4] The $\simeq$10% higher sensitivity of the image plate[15] for $K\alpha_2$ photons than to $K\alpha_1$ radiation results in a 10% discrepancy.

A similar discrepancy is found in the filtered $K\alpha$ lines. Both the 0.25 mm thick Hf filter and the 0.1 mm thick Ta filter transmit a larger fraction of the $K\alpha$ lines than expected. Dose enhancement on the interface between a high atomic number filter and a lower atomic number diagnostic might contribute to the discrepancy and is a topic for further study.

Reading the BAS-SR image plate exposed half a day to a nominally 34 kBq radioactive ^{109}Cd source 32 mm away, 1.5×10^5 photons per mm^2, gives a pixel value around 300. Fading over the exposure time and correcting for the ratio between the mass absorption coefficients for ^{109}Cd's 88 keV photons and 59 keV $K\alpha_1$ radiation suggests an approximate calibration: if the spectra are read shortly after exposure (as they were), a pixel value of 1000 corresponds to 0.15×10^5 $K\alpha_1$ photons per mm^2, or a fluence $F\simeq1.5$ nJ/mm^2. The pixel value averaged over the $K\alpha_1$ line, about 600, then means 1 nJ/mm^2: each $K\alpha_1$ photon increases the pixel value of a 50 μm by 50 μm pixel by about 3.

All the 200 $K\alpha_1$ photons per pixel must arrive in less than the electrical pulse length $\Delta t\simeq50$ ns. The average flux $F/\Delta t$ is then about 4 $K\alpha_1$ photons per nanosecond. Although the arrival time is undoubtedly shorter and the peak flux is undoubtedly higher, spatially and time-resolved data desired in the future must balance resolution with signal to noise.

At the $K\alpha_1$ photon energy the image plate's active medium, $Ba_{1.85}I_{0.15}F$, has a mass attenuation coefficient $(\mu/\rho)\simeq6$ cm^2/g. A 1.5 nJ/mm^2 fluence F then produces about $D=(\mu/\rho)F\simeq1$ mGy in dose. A BAS-SR image plate exposed to this dose in pulsed electrons gives similar pixel values: 350 on one reader, and 1200 on another.[16]

Figure 5 is for nominally the same shot as in Fig. 3, but with much lower background thanks to a thinner vacuum window, shielding of the window against irradiation on the vacuum side, and improved shielding of the spectrometer against scattered radiation. On the top right side the $K\alpha_1$ line passes through the 0.1 mm thick Tm filter (top square) the same way as the lower-energy $K\alpha_2$ line, showing that the $K\alpha_1$ photons from the PFRP's ionized tungsten remain within 0.07 keV of the 59.318 keV energy of neutral tungsten. The 0.25 mm thick Hf filter in the middle suppresses all the $K\beta$ lines, and the 0.1 mm or 0.2 mm thick Ta filter suppresses the $K\beta_2$ line. The two exposures on the left side can be directly compared: the larger one is from a 70 mm wide BAS-MS image plate, the smaller one in the middle left is from a Hamamatsu S8985–02 CCD designed for dental imaging. On all these images the fluorescence lines stand out clearly thanks to a much lower background.

Figure 6 compares the tungsten spectra on the left side in Fig. 5, from BAS-SR image plate and the S8985 CCD. The line intensity relative to the background is approximately the same in both registration media, and the image plate's 16-bit resolution accounts for almost all of its order of magnitude larger pixel value than the 12-bit CCD. Otherwise, the spectra are substantially identical, both the actual line shapes and the spatially integrated versions that made the exposures overlap when multiplied by 9.6. The line shapes on the CCD are analyzed in more detail elsewhere.[11]

The $K\alpha_1$ line has a peak of 3500, in units of pixel value. Integrating over the line gives 1500, in units of pixel value-millimeter. The image plate's calibration above suggests that this line intensity requires 2.25×10^5 $K\alpha_1$ photons per millimeter along the spectral line. The integrated reflectivity at 59 keV of $20\bar{2}3$ quartz is estimated as $\simeq3\times10^{-5}$. On the image plate 1200 mm from the x-ray source, a 1 mm long section of the $K\alpha_1$ line receives all the photons emitted by the source into a $\simeq3\times10^{-8}$ sr solid angle. The fluence in $K\alpha_1$ photons per steradian at the source is then approximately 7.5×10^{12}.

The photon fluence can also be obtained from the data in Weber *et al.*[3] Their Fig. 15 shows the energy spectrum of the 2.5×10^{17} electrons in the discharge's 40 mC. Per electron, the computed spectrum in their Fig. 17 contains 4×10^{-3} $K\alpha_1$, $K\alpha_2$, and combined $K\beta$ photons per steradian in the forward direction, for an expanded plasma that matches their differential filter data. The dose calculated from this spectrum is four times larger than what is measured, suggesting that the active number of electrons is 6×10^{16} with a charge of 10 mC. The computation then gives 2.4×10^{14} K-line pho-

tons per steradian. Half of these are $K\alpha_1$ photons, or about 1.2×10^{14} $K\alpha_1$ photons per steradian. Given the various approximations the factor-16 discrepancy between the two estimates seems tolerable.

III. CONCLUSION

The primary purpose in this work is to develop a crystal spectrometer with at least 0.06 keV resolution at around 60 keV that works in a hard bremsstrahlung environment, to be extended later on to 0.03 keV resolution. Such high resolution has not yet been reached. However, the bremsstrahlung background has been properly suppressed by shielding against scattered radiation from the vacuum window or other scatter sources that could send undiffracted photons along the same path as the diffracted photons.

The fluorescence from Gamble II's PFRP is strong enough that the x-rays could be observed farther away from the bent crystal, preferably on the Rowland circle by bending the crystal to a larger radius. A crystal with smaller $2d$ spacing and larger dispersion could work even in the present geometry if its reflectivity is sufficiently high. More expensive approaches to be contemplated for the future include an x-ray sensor with improved spatial and time resolution, undoubtedly with the necessary amplification. To see whether this is possible with the PFRP, the crystal's throughput and the image plate or CCD must be measured quantitatively.

ACKNOWLEDGMENTS

This work was supported through Contract No. W911QX09D0016 with the Army Research Laboratory, and by DTRA's Basic Research Sciences MIPR 08-2468 and MIPR 09-2156 with the Naval Research Laboratory. The expert handling of the PFRP and Gamble II by E. Featherstone and D. Phipps is gratefully acknowledged.

[1] R. A. Mahaffey, J. Golden, S. A. Goldstein, and G. Cooperstein, Appl. Phys. Lett. **33**, 795 (1978).
[2] B. V. Weber, R. J. Commisso, G. Cooperstein, D. D. Hinshelwood, D. Mosher, P. F. Ottinger, D. M. Ponce, J. W. Schumer, S. J. Stephanakis, S. B. Strasburg, S. B. Swanekamp, and F. C. Young, Phys. Plasmas **11**, 2916 (2004).
[3] B. V. Weber, R. J. Allen, R. J. Commisso, G. Cooperstein, D. D. Hinschelwood, D. Mosher, D. P. Murphy, P. F. Ottinger, D. G. Phipps, J. W. Schumer, S. J. Stephanakis, S. C. Pope, J. R. Threadgold, L. A. Biddle, S. G. Clough, A. Jones, M. A. Sinclair, D. Swatton, T. Carden, and B. V. Oliver, IEEE Trans. Plasma Sci. **36**, 443 (2008).
[4] See http://xdb.lbl.gov for section 1 in the X-Ray Data Booklet.
[5] L. T. Hudson, R. D. Deslattes, A. Henins, C. T. Chantler, E. G. Kessler, and J. E. Schweppe, Med. Phys. **23**, 1659 (1996).
[6] L. T. Hudson, R. Atkin, C. A. Back, A. Henins, G. E. Holland, J. F. Seely, and C. I. Szabo, Radiat. Phys. Chem. **75**, 1784 (2006).
[7] J. F. Seely, G. E. Holland, L. T. Hudson, C. I. Szabo, A. Henins, H.-S. Park, P. K. Patel, R. Tommasini, and J. M. Laming, High Energy Density Phys. **3**, 263 (2007).
[8] M. S. Litz, G. Merkel, N. R. Pereira, C. N. Boyer, G. E. Holland, J. W. Schumer, J. F. Seely, L. T. Hudson, and J. J. Carroll, Phys. Plasmas **17**, 043302 (2010).
[9] C. D. Chen, J. A. King, M. H. Key, K. U. Akli, F. N. Beg, H. Chen, R. R. Freeman, A. Link, A. J. Mackinnon, A. G. MacPhee, P. K. Patel, M. Porkolab, R. B. Stephens, and L. D. Van Woerkom, Rev. Sci. Instrum. **79**, 10E305 (2008).
[10] J. F. Seely, L. T. Hudson, G. E. Holland, and A. Henins, Appl. Opt. **47**, 5753 (2008).
[11] J. F. Seely, N. R. Pereira, B. V. Weber, J. W. Schumer, J. P. Apruzese, L. T. Hudson, C. I. Szabo, and C. N. Boyer, "Spatial resolution of a hard x-ray CCD detector," Appl. Opt. (submitted).
[12] J. F. Seely, L. T. Hudson, G. E. Holland, and A. Henins, Appl. Opt. **47**, 2767 (2008).
[13] N. R. Pereira, G. Merkel, and M. S. Litz, Laser Phys. **17**, 874 (2007).
[14] E. O. Baronova, M. M. Stepanenko, and N. R. Pereira, Rev. Sci. Instrum. **72**, 1416 (2001).
[15] N. Izumi, R. Snavely, G. Gregori, J. A. Koch, H.-S. Park, and B. A. Remington, Rev. Sci. Instrum. **77**, 10E325 (2006).
[16] K. Zeil, S. D. Kraft, A. Jochmann, F. Kroll, W. Jahr, U. Schramm, L. Karsch, J. Pawelke, B. Hidding, and G. Pretzler, Rev. Sci. Instrum. **81**, 013307 (2010).